

# Comparing Of Application Analysis Program with Experimental Studying to Repair Steel Pipe by Composite Materials for Industry

Mohamed A.Higaeg<sup>1</sup>, Zamzam.A.Elsharif<sup>2</sup>, Bashir.M.Gallus<sup>3</sup>, Elmabruk S. Shwaikha<sup>4</sup>, and Awad I.Zableh<sup>5</sup>  
 Mechanical Dep<sup>1,2,3,5</sup>. College of Technical Sciences Misurata<sup>1,2,3,5</sup>, Industrial Dep<sup>4</sup>. Higher Institute for Sciences  
 Techonlogy/Misurata<sup>4</sup>

Misurata- Libya

Email: mhigaeg@gmail.com<sup>1</sup>, zamzamalsharif@hotmail.com<sup>2</sup>, bashir.bashir11311@gmail.com<sup>3</sup>, m.Shwaikha@gmail.com<sup>4</sup>, Zblah66@gmail.com<sup>5</sup>.

**Abstract**— This paper presents theoretical studying about simulation between application finite element analysis program (FEA) with previous results and data about defected damaged area of module steel pipes. Experimental studying was based on previous papers and books [1,2] that were discussion the module which was simulated as circular corrosion crack at the middle of the pipes which were made from carbon steel (Steel-No DIN10421) with internal diameter of 83 mm, thickness 12.5 mm and length of 900 mm .The damaged area of circular was simulated at diameters 5,10,15 mm, and 20 mm for the four pipes respectively[1,2]. Also, manufacturing composite material was used of repair the fiber glass woven roving (type E) at  $[0^{\circ}/90^{\circ}/\pm 45^{\circ}]_s$  reinforced with polyester resin. A carbon steel bolted clamp was used to clamp the pipe around the defected holes to minimize the delamination effect and stop the leakage of water during the tests of the pipes [1,2]. The finite element analysis program: CATIA V5 based on apply inner pressure about defected damaged area at diameter 10 mm of pipe to evaluate the deflection, failure pressure (blister pressure) and stress-strain curves.

It has fund that good correlations between the finite element analysis (FEA) of radial strain with previous studying curves at stages of loading of pressure. Also, observed the finite element analysis (FEA) curve was lowest radial strain of failure comparing with previous studying curves of crack length 10 mm at  $957.730 \mu\epsilon$  while highest radial strain was theoretical model radial strain at  $1389.430 \mu\epsilon$  of pressure. According to studying the experimental curve and the finite element curve exhibited the non-linearity only in the early stages and then became linear up to failure. The finite element analysis (FEA) curve was highest radial stress of failure comparing with previous studying curves of crack length 10 mm at 46.541 MPa while radial stress of previous studying were 32.6941 MPa. Good correlation between the finite element analysis (FEA) and

theoretical model of blister deflection. The finite element analysis (FEA) was higher of blister deformation then theoretical model  $22.9490 \mu\text{m}$  and  $6.7014 \mu\text{m}$  respectively. Finally, The maximum blister deflection occurs at the centre of the hole (crake length 10 mm) by finite element analysis (FEA).

**Keywords**—Finite element analysis (FEA); Composite materials; steel pipes; defected damaged area; clamp; quasi-isotropic laminate; Blister pressure; Deformation; Rehabilitation; failure mode; stress and strain.

## I. INTRODUCTION

Steel pipelines are increasingly used for a variety of applications, such as in the oil, gas and high pressure container industries. Operating steel pipe in cruel environmental conditions can expose it to a variety of damage types such as erosion, corrosion, and mechanical damage [3-5].

Damage is the main cause of crack initiation, and so bonded composite repair can be used to prevent leakage and restore all or part of the maximum allowable operating capacity of the pipeline. Furthermore, fiber reinforced polymer (FRP) materials are highly suited for use as repair material, as they possess a very high specific strength and stiffness, a high formability, an inherent immunity to corrosion, and ease of fabrication [6]. A number of studies have investigated pipeline with bonded composite patches, notably [7], [8], API [9], ASME [10] and [11].

Failure analysis of pipe made of glass-reinforced plastic with an inclined surface crack under static internal pressure was investigated by [12]. He concluded that, the crack propagation occurred in Mode II. He mentioned that, the critical stress intensity factor according to mixed mode must be determined in order to study the failure of pipe with crack. [8] developed a composite repair system of steel pipeline, formed from unidirectional fibers wrapped in the circumferential direction of the pipe. Moreover, they deduced a formula to calculate the sufficient thickness

of the repair wrap, depending on the ultimate tensile strength of the steel pipe and the ultimate tensile strength of the repair wrap. also developed an integrated analytical and experimental method to evaluate the integrity of an onshore composite repair technique. They used a carbon/epoxy- based composite system as a repair for steel pipe. [7] studied the response of repaired pipelines under internal pressure, axial force, and bending. [13] also used glass-reinforced polymer to repair steel pipelines based on strain-based design. They found good agreement between their experimental and numerical results. They concluded that the optimized design of composite repaired steel pipelines depends on the fiber orientation of composite repair. The prediction of fracture parameters such as  $J$ -integral, stress intensity factors (SIF), and failure strength is one of the most important aspects in the design of composite repair. Recently, many researchers have concentrated about this point.[14] were studied the effect of stitched reinforcements on impact-induced damage and damage propagation under flexural load with TiNi and Kevlar as the superelastic element and the reference thread, respectively. In addition to finite element model. They Showed that Unstitched carbon/epoxy laminates were also produced. Embedded damage (matrix cracks, fiber rupture and delamination) was induced by low velocity impact testing. Simulated the propagation of damage, and particularly delamination, in stitched and unstitched structures during the bending test, and, depending on the mechanical properties of the stitching threads, different propagation schemes by finite element analysis (FEA). [15] were studied Effectiveness of using fiber-reinforced polymer composites for underwater steel pipeline repairs. [16] were studied the effectiveness of a new composite laminate for the pipes repair which showed First, the mechanical and thermal properties of the new developed composite laminate. Next, two defect types, Type A (non-through wall) and Type B (through wall) that were manufactured into the pristine pipe specimen and the evaluation of the performance of the repaired pipe that was carried out by hydrostatic tests. They were obtained to The performance of the repaired pipe using the new developed composite laminate material was satisfactory in both defect types. [17] were studied experimental and numerical fatigue crack growth of an aluminium pipe repaired by composite patch which presented fatigue crack trajectory and also the crack growth curves versus number of cycles of load and showed validation of results is then achieved through the extended finite element method (XFEM).In addition, a stand-alone MATLAB programming package was developed to study such structures with 3D degenerated shell elements. They observed that the cracked pipe was finally repaired by glass/epoxy polymer composite and the effect of the patch on the extension of fatigue life through experimental tests and the XFEM framework. [18] were studied the efficiency of the glass fiber reinforced polymer patch for repairing cracked steel pipe subjected to internal pressure. The effect of fiber

orientation,  $[0_0]_{8s}$ ,  $[90_0]_{8s}$ , and  $[0_0/90_0]_{4s}$ , of bonded composite repair on reducing  $J$ -integral of stationary crack with different inclination angles ( $\theta$ ) was studied using the 3-D finite element method, FEM. Extended-FEM had been adopted to simulate the crack growth of different inclined stationary cracks in steel pipe subjected to internal pressure. They found that, the growing crack emanated from inclined stationary crack switched its path to be under pure mode I. The crack initiation pressure of inclined stationary crack in steel pipe with composite repair is higher than that of pipe without composite repair. The composite repair reduced the value of  $J$ -integral of stationary crack in steel pipe. This reduction is strongly affected by the crack length and ( $\theta$ ) of the stationary crack and it is fairly affected by the fiber orientation.[19] were presented that a four-phase program to improve the pressure capacity of internally pressurized composite overwrapped damaged metallic pipes was undertaken. In the first phase, designing, fabricating of automated cost-effective composite repair system was carried out. The second phase focuses on the effects of composite overwrapped metallic pipes to understand the influence of fabric orientation angle on their responses of to the internal pressure. Phase three evaluates the improvement in pressure capacity of overwrapped damaged pipes by varying the fabric orientation. The fourth phase is devoted to investigate the corrosion resistance of the pipes. They obtained to the fabric orientation of composite overwrapped exhibited a pronounced effect on the damaged pipes capability to carry high internal pressure. Composite overwrapped damaged metallic pipes exhibited high pressure capacity compared with externally damaged and non-damaged metallic pipes.

In this paper, finite element analysis program (FEA) will be applied at middle defected damaged area is 10mm to composite repair steel pipe. It will be compared with previous experimental investigating as results and data to evaluate deformation with blister pressure, pressure –radial strain, and radial stress-strain curve.

II. THEORETICAL SET-UP.

A. Geometry and Mechanical Properties of composite Materials.

In present work the three-dimensional finite element model for composite repaired steel pipe consists of the pipe and E-glass fiber (type: woven roving ) at  $[0^\circ/90^\circ/\pm 45^\circ]_s$  reinforced polyester GFRP composite repair. The geometry of composite repaired steel pipe was selected based on [1,2] as shown Fig.1. Table shows mechanical properties of composite materials laminate that selected on [1,2].

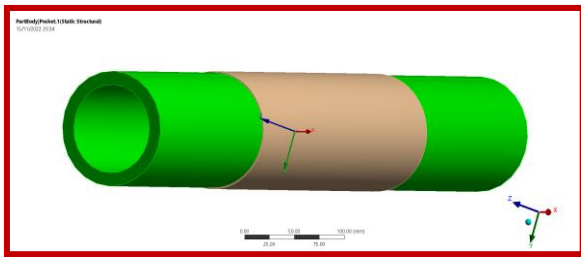


Fig. 1 Three-dimensional of steel pipe with composite repair laminate.

TABLE I. Material properties of fiber glass, resin [1,2].

<b>Modulus of elasticity (E) of composite</b>	15.768 $GP_a$
<b>Shear modulus (G) of the composite</b>	5.73 $GP_a$
<b>Poisson's ratio of composite laminate</b>	0.376
<b>Volume fraction</b>	0.41
<b>Overall thickness</b>	4.25 mm
<b>Defected Hole</b>	10 mm
<b>Number of plies</b>	8
<b>Warped angles</b>	$[0^\circ/90^\circ/\pm 45^\circ]_s$
<b>Elastic Modulus of resin (<math>E_m</math>)</b>	4 $GP_a$
<b>Elastic modulus of fiber</b>	72 $GP_a$
<b>Density of the composite laminate</b>	1.9 g/cc
<b>Density of the glass fiber</b>	2.5 g/cc
<b>Density of the matrix</b>	1.3 g/cc

B. Composite Materials Mesh.

Fig.2 shows mesh repair laminate of 3-D elastic FE model has been developed using the CATIA5 program to account for the geometric and material behavior of composite repaired steel pipe, which the mesh sizing 2 mm and consisted of 274594 elements and 321606 nodes. Also, it has been used to simulate the fracture crack path in various crack analysis problems (fracture mechanics) with different fiber orientation in steel pipe. Table II, extracted from previous studying [1,2] that has been based on

classification laminate theory (CLT). Mechanical properties of repair laminate, the engineering constants, the coefficient stiffness matrix and the Compliance Matrices. Thus, the stiffness characteristics of a symmetric quasi-isotropic laminate, observed from previous studying [1,2]. In addition, there are no mesh cells under an orthogonal quality of 0.078748 or over a skews of 0.98195.

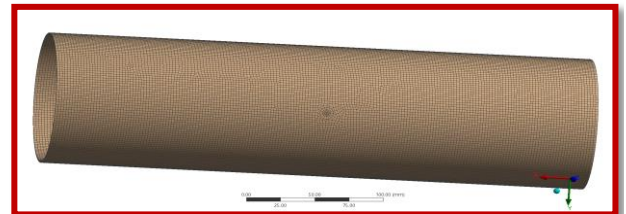


Fig. 2 Three-dimensional mesh of composite repair laminate.

TABLE II. laminate properties for E-glass/polyester  $[0^\circ/90^\circ/\pm 45^\circ]_s$  [1].

Symbol	Value	Property
$E_{11} GP_a$	32.044	Young's modulus in fiber direction
$E_{22} GP_a$	10.431	Young's modulus in the transverse direction
$E_x GP_a = E_y GP_a$	15.768	Young's modulus of repair laminate in the xy plane
$\nu_{12}$	0.31	Poisson's ratio for unidirectional ply in the material principal direction
$\nu_{21}$	0.101	Poisson's ratio for unidirectional ply in the material principal direction
$\nu_{xy} = \nu_{yx}$	0.376	Poisson's ratio of repair laminate in the xy plane.
$G_{12} GP_a$	2.168	In- plane shear modulus
$G_{xy} GP_a$	5.73	Shear module of repair laminate in the xy plane.
$t_s mm$	1.2	Repair symmetric thickness
$A_{11} MP_a$	22.0338	Extensional stiffness of repair laminate
$A_{12} MP_a$	8.2806	Extensional stiffness of repair laminate
$A_{22} MP_a$	22.0338	Extensional stiffness of repair laminate
$A_{16} MP_a$	0.0	Extensional stiffness of repair laminate
$A_{26} MP_a$	0.0	Extensional stiffness of repair laminate
$A_{66} MP_a$	6.8766	Extensional stiffness of repair laminate

$D_{11}$ N. mm	3.4807	Bending stiffness of repair laminate
$D_{12}$ N. mm	0.6089	Bending stiffness of repair laminate
$D_{22}$ N. mm	2.577	Bending stiffness of repair laminate
$D_{16}$ N. mm	0.0573	Bending stiffness of repair laminate
$D_{26}$ N. mm	0.0573	Bending stiffness of repair laminate
$D_{66}$ N. mm	0.4404	Bending stiffness of repair laminate
AA MP <sub>a</sub>	416.92	equivalent membrane elastic constants
$a_{11}$ 1/MP <sub>a</sub>	0.05285	Compliance matrices of repair laminate
$a_{12}$ 1/MP <sub>a</sub>	0.01986	Compliance matrices of repair laminate
$a_{22}$ 1/MP <sub>a</sub>	0.05285	Compliance matrices of repair laminate
$a_{66}$ 1/MP <sub>a</sub>	0.1454	Compliance matrices of repair laminate

C. Contact and loading regime.

Fig.3 shows Pressure was loaded inside the pipe surface,  $P$ , at 2,3,4,5,8,11,13,16 and 18 MPa [1]. In the present model is used to simulate the contact properties of crack surface (defected damaged area) which were applied between the outer surface of pipe and inner surface of composite repair as a tie contact.

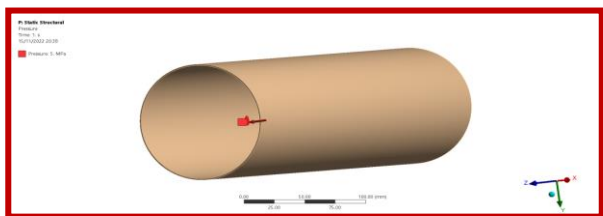


Fig. 3 Three-dimensional inner pressure of composite repair laminate.

III. RESULTS AND DISCUSSION.

The results which were observed of the pipe with defect length of 10 mm by FEA at varies pressures as shown in Fig.4. Also, Tables III-V information summary of Preliminary study [1,2] and present work in order to comparing between radial strain, deflection, and stress- strain curves.

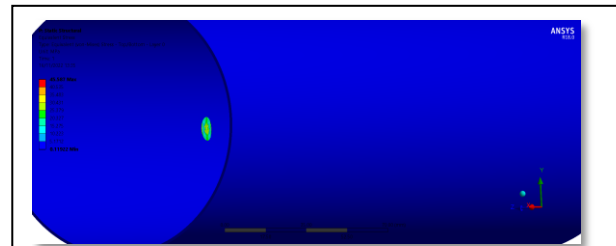


Fig.4-a. 3D at  $P_i = 2MPa$  and crack length 10mm

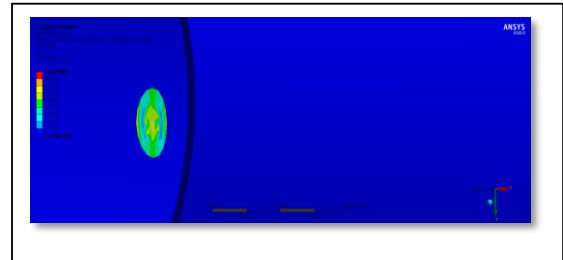


Fig.4-b. 3D at  $P_i = 3MPa$  and crack length 10mm

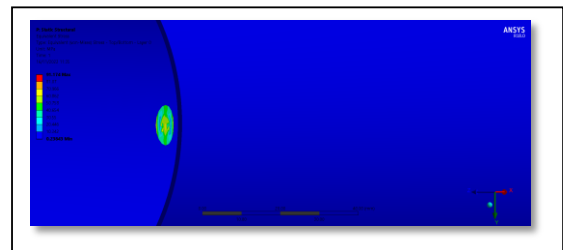


Fig.4-c. 3D at  $P_i = 4MPa$  and crack length 10mm

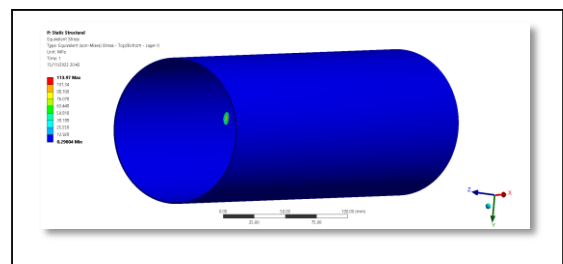


Fig.4-d. 3D at  $P_i = 5MPa$  and crack length 10mm

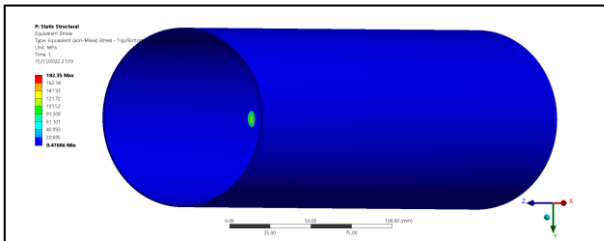


Fig.4-e. 3D at  $P_i = 8MPa$  and crack length 10mm

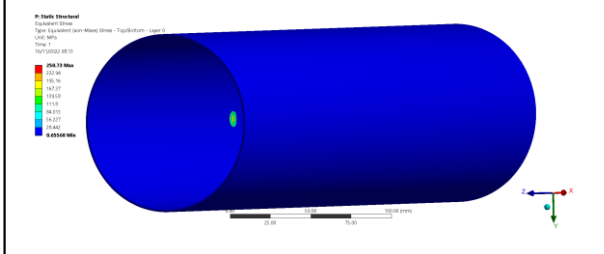


Fig.4-f. 3D at  $P_i = 11MPa$  and crack length 10mm

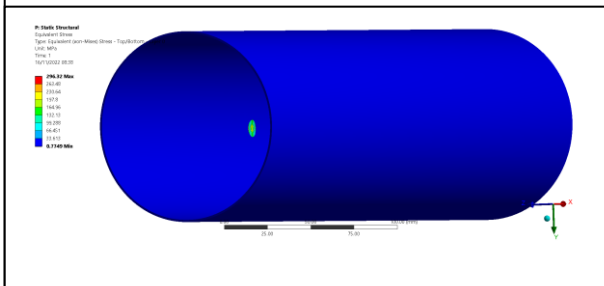


Fig.4-g. 3D at  $P_i = 13MPa$  and crack length 10mm

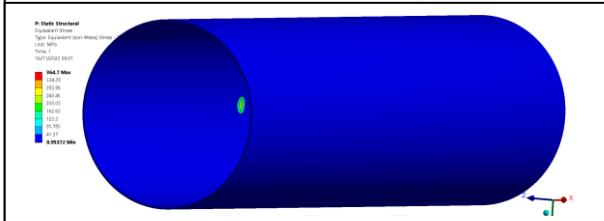


Fig.4-h. 3D at  $P_i = 16MPa$  and crack length 10mm

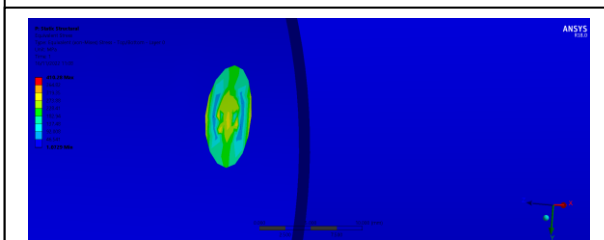


Fig.4-i. 3D at  $P_i = 18MPa$  and crack length 10mm

Fig. 4 Effect the inner pressure on defected damaged area of composite repair( crack length) inter steel pipe by FEA .

TABLE III. Pressure – Radial strain for defected area with 10mm.

Pressure $MPa$	Redial strain (FEA) $\epsilon_r, \mu\epsilon$	Theoretical radial Strain $\epsilon_r, \mu\epsilon$	Expermental radial strain $\epsilon_r, \mu\epsilon$
2	106.410	154.381	80.0
3	209.620	231.572	170.0
4	212.830	308.762	210.0
5	266.040	385.953	260.0
8	425.660	617.525	440.0
11	585.280	849.096	610.0
13	691.690	1003.478	770.0
16	851.310	1235.049	960.0
18	957.730	1389.430	1130.0

TABLE IV. Redial stress – Radial strain for defected area with 10mm.

Redial stress(FEA) $MPa$	Redial strain(FEA) $\epsilon_r, \mu\epsilon$	Redial stress $\sigma_r, MPa$	Theoretical radial Strain $\epsilon_r, \mu\epsilon$	Theoretical radial Strain $\epsilon_r, \mu\epsilon$
5.171	106.410	3.63268	154.381	80
7.757	209.620	5.44902	231.572	170
10.342	212.830	7.26536	308.762	210
12.928	266.040	9.0817	385.953	260
20.685	425.660	14.5307	617.525	440
28.442	585.280	19.9798	849.096	610
33.613	691.690	23.6124	1003.478	770
41.370	851.310	29.0615	1235.049	960
46.541	957.730	32.6941	1389.430	1130

TABLE V. Pressure – Deflection for defected area with 10mm.

Pressure $MPa$	Deflection (FEA) $y, \mu m$	Blister deflection $y, \mu m$
2	2.5499	0.7446
3	3.8249	1.1169
4	5.0998	1.4892
5	6.3748	1.8615
8	10.20	2.9784
11	14.0240	4.0953
13	16.5740	4.8399
16	20.3990	5.9568
18	22.9490	6.7014

Figure 5 shows the comparison between the propagation of experimental pressurized blister ( $MP_a$ ) versus finite element analysis, theoretical and experimental radial strain ( $\mu\epsilon$ ) curves [1,2] those defected area( crack length) of hole 10mm . The theoretical radial strain were calculated using the model which was developed in the part one of this work [1,2]. It can be noted that all the curves exhibited the same manner. The curves are linearity behavior up to failure. Good correlations between the finite element analysis of radial strain and previous studying curves can be observed at stages of loading. In addition, it can observed that finite element analysis curve was lowest strain of failure comparing with previous studying curves of crack length 10 mm at  $957.730 \mu\epsilon$  while highest strain was theoretical radial strain at  $1389.430 \mu\epsilon$  and pressure 18MPa.

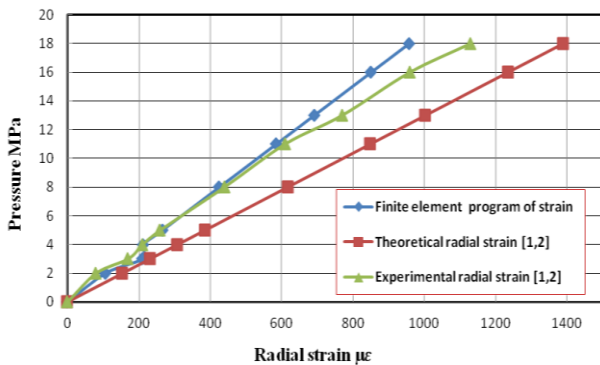


Fig. 5 Comparing between propagation of pressure versus finite element analysis, previous studying of radial strain with defected area 10 mm .

Figure 6 shows the comparison between the radial stress - strain curves for finite element model, fracture mechanics model (theoretical) and experimental test [1,2]. The finite element model was developed by finite element program: CATIA V5 . The fracture mechanics model was developed by fracture mechanics and composite lamina theory as mentioned in the previous studying [1,2]. It can be demonstrated that the experimental curve and the finite element curve exhibited the non-linearity only in the early stages and then became linear up to failure. The fracture mechanics model is linear up to failure. The non-linearity of the experimental curve is probably related to the matrix cracking through the thickness of the composite layers. The non-linearity due to matrix cracks is well documented in the literature [20-22]. The immediate effect of micro cracks is to cause degradation of the stiffness due to redistribution of stresses and variation of strain in cracked laminate [23]. The matrix cracks can induce delamination which leads to fibre breakage or provides pathways for the entry of pressurised liquid between the layers and may lead to laminate failure. Good correlations between the three curves can be observed at stages

of loading. In addition, it can observed that finite element analysis curve was highest radial stress of failure comparing with previous studying curves of crack length 10 mm at 46.541 MPa while radial stress of previous studying were 32.6941 MPa.

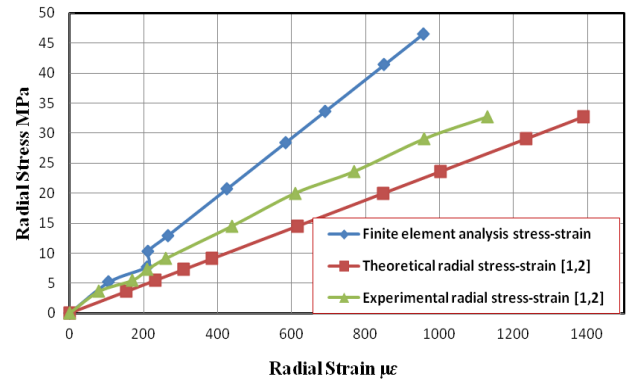


Fig. 6 Comparing between radial stress-strain versus finite element analysis, previous studying with defected area 10 mm .

Figure 7 shows the comparison between the propagation of experimental pressurized blister  $MP_a$  and blister deformation  $\mu m$  (deflection) curves for finite element analysis (FEA) and theoretical model [1,2]. The deformation model was developed by fracture mechanics which calculated in the part one of this work [1]. It can be noted that all the curves exhibited the same manner . The finite element and theoretical model are linear up to failure. However, there were finite element was higher at blister deformation then theoretical model  $22.9490 \mu m$  , and  $6.7014 \mu m$  respectively at pressure 18MPa that one previous studying was used clamped steel around defected area to minimum delamination and to obtain high efficiency of repair.

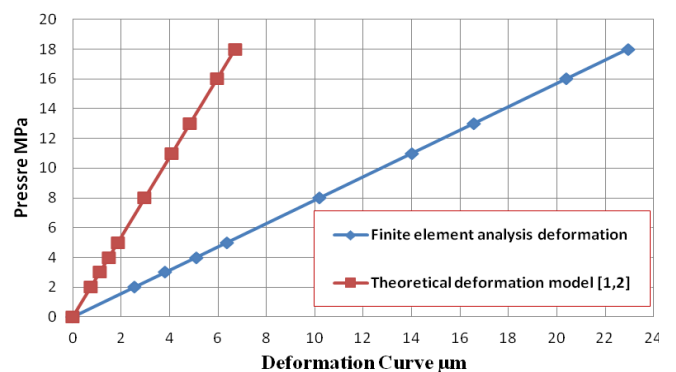


Fig. 7 Comparing between pressure and deformation versus finite element analysis and previous studying with defected area 10 mm .

Figure 8 shows an example to apply FEA of the distribution the elemental deflection over repaired area under pressure loading at 18MPa. It can be seen that the maximum blister deflection occurs at the centre of the hole then decreases towards the edges of the hole in radial direction.

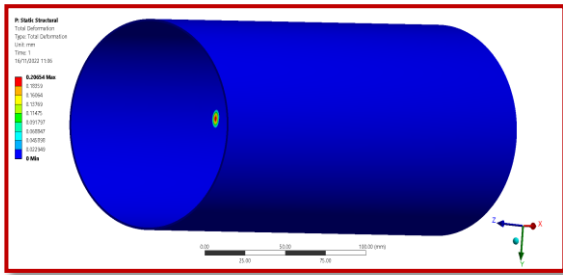


Fig. 8 The distribution of finite element deflection over the defected area 10 mm.

#### IV. CONCLUSION.

- The work shows that it is possible to apply finite element analysis (**FEA**) for external repair of metal piping system.
- Good correlations between the finite element analysis (**FEA**) of radial strain with previous studying curves at stages of loading of pressure.
- The finite element analysis (**FEA**) curve was lowest radial strain of failure comparing with previous studying curves of crack length 10 mm at  $957.730 \mu\epsilon$  while highest radial strain was theoretical model radial strain at  $1389.430 \mu\epsilon$  of pressure.
- Good correlations between the finite element analysis (**FEA**) of radial stress- strain curve with previous studying at stages of loading of pressure.
- The finite element analysis (**FEA**) curve was highest radial stress of failure comparing with previous studying curves of crack length 10 mm at 46.541 MPa while radial stress of previous studying were 32.6941 MPa.
- Good correlation between the finite element analysis (**FEA**) and theoretical model of blister deflection.
- The finite element analysis (**FEA**) was higher of blister deformation then theoretical model  $22.9490 \mu m$  and  $6.7014 \mu m$  respectively.
- The maximum blister deflection occurs at the centre of the hole (crack length 10 mm) by finite element analysis (**FEA**).

- A good convergence results of static structural with reducing the iterations and less error.
- The quality average of orthogonal and skews were 0.98457 and 0.0.04291 respectively.

#### REFERENCE

1. Zamzam A. Alsharif. Design Model of Damaged Steel Pipes for Oil and Gas Industry Using Composite Materials. Part II: Modelling. A.Ochsner and H.Ahenbach (ed). Design and Computation of modern Engineering Materials, Advanced structured Materials 54, DOI: 10.1007/978-3-319-07383-5-12, © Springer International publishing Switzerland 2014.
2. Zamzam ELsharif.: Repair of Damaged Metal Pipes Using By Composite Materials. LAP LAMBERT Academic Publishing. ISBN: 978-3-659-75975-8, Deutschland-Germany, 2015.
3. El-Bagory, T.M., Younan, M., Sallam, H.E.M., Abdel-Latif, L. 2013. Plastic load of precracked polyethylene miter pipe bends subjected to in-plane bending moment. JPVT 35, 061203, 9 pp.
4. El-Bagory, T.M., Sallam, H.E.M., Younan, M. Effect of strain rate, thickness, welding on the J-R curve for polyethylene pipe materials. Theor Appl Fract Mech 74. 164-180 , 2014.
5. El-Bagory, T.M., Sallam, H.E.M., Younan, M. Evaluation of Fracture Toughness Behavior of Polyethylene Pipe Materials”, JPVT, 137(6), 061402, 10 pp, 2015.
6. Baker A. Bonded composite repair of fatigue-cracked primary air craft structure. Compos Struct.,47, 431–43,1999.
7. Shouman A, Taheri F. An investigation into the behaviour of composite repaired pipelines under combined internal pressure and bending. In: Proceedings of the ASME 28th international conference on ocean, offshore and arctic engineering, Honolulu, Hawaii ,2009.
8. Alexander C, Ochoa O. Extending Onshore Pipeline Repair to Offshore Steel Risers with Carbon-Fiber Reinforced Composites. J Compos Struct 92, 499–507 ,2010.
9. API 5L. Specification for line pipe. APL specification 5L, 42nd ed. USA: The American Petroleum Institute , 2000.
10. ASME PCC2. Repair of pressure equipment and piping standard. 2006 ed. New York (NY): ASME ,2006.
11. Köpple M.F, Lauterbach S., Wagner W. Composite repair of through-wall defects in pipe work – Analytical and numerical models with respect to ISO/TS 24817. Composite Structures, 95, 173–178 , 2013
12. Arikan H. Failure analysis of ( $\pm 55^\circ$ )<sub>3</sub> filament wound composite pipes with an inclined

- surface crack under static internal pressure. *Composite Structures* 92, 182–187, 2010.
13. Shouman A, Taheri F. Compressive strain limits of composite repaired pipelines under combined loading states. *Composite Structures*, 93, 1538–1548, 2011.
  14. [Pierre L.V.](#), [Vladimir B.](#), [Patrick T.](#) Impact-induced damage and damage propagation under flexural load in TiNi and Kevlar-stitched carbon/epoxy laminates. *Composite Structures*, Vol.100, PP 424-435, June 2013.
  15. [Shamsuddoha M.d.](#), [Mainullislam M.d.](#), [Thiru A.](#), [Allan M.](#), [Kin T.](#) Effectiveness of using fibre-reinforced polymer composites for underwater steel pipeline repairs. *Composite Structures*, Vol.100, PP 40-54, June 2013.
  16. [Rohem N.R.F.](#), [Pacheco L.J.](#), [Budhe S.](#), [Banea M.D.](#), [Sampaio E.M.](#), [Barros S.de.](#) Development and qualification of a new polymeric matrix laminated composite for pipe repair. *Composite Structures*, Vol. 152, PP 737-745, 15 September 2016.
  17. [Zarrinzadeh H.](#), [Kabir M.Z.](#), [Deylami A.](#) Experimental and numerical fatigue crack growth of an aluminium pipe repaired by composite patch. *Engineering Structures*, Vol.133, PP 24-32, 15 February 2017.
  18. Amr A.A. Hossam E.M.S., Muhammad A.M. Failure Analysis of Composite Repaired Pipelines with an Inclined Crack under Static Internal Pressure. ScienceDirect., *Procedia Structural Integrity* 123–130, May 2017. [www.sciencedirect.com](http://www.sciencedirect.com).
  19. [Mahdi E.](#), [Eltai E.](#) Development of cost-effective composite repair system for oil/gas pipeline. *Composite Structures*, Vol.202, PP. 802-806, 15 October 2018. <https://doi.org/10.1016/j.compstruct.2018.04.025> Get rights and content.
  20. Petit, P.H. and Waddoups, M.E., " Method of predicting the Non linear Behaviour of Laminated Composite", *Journal of Composite Materials*, Vol. 3, 1969, pp. 2-19.
  21. Nahas, M.N., " Analysis of Non linear Stress-strain Response of Laminated Fibre Reinforced Composite", *Fibre Science and Technology*, Vol. 20, 1984, pp. 297-313.
  22. Saied, R.O., and Shuaeib, F.M., " Modelling of the Nonlinearity of Stress-Strain Curves for Composite Laminates, *Journal of Engineering Research*, Issue 7, March 2007, pp. 1-14.
  23. Talreja, R., " Transverse Cracking and Stiffness Reduction in Composite Laminates, *Journal of Composite Materials*, Vol. 19, 1985, pp. 355-375.